JOURNAL OF VIROLOGY, June 2000, p. 5729–5735 Vol. 74, No. 12
0022-538X/00/$04.00+0

Impact of Human Immunodeficiency Virus Type 1 RNA Dimerization on Viral Infectivity and of Stem-Loop B on RNA Dimerization and Reverse Transcription and Dissociation of Dimerization from Packaging

NI SHEN,[1,2] LOUIS JETTÉ,[1] CHEN LIANG,[1] MARK A. WAINBERG,[1,3] AND MICHAEL LAUGHREA[1,2]*

McGill AIDS Centre, Lady Davis Institute for Medical Research, Sir Mortimer B. Davis-Jewish General Hospital,[1] and Department of Medicine[2] and Department of Microbiology and Immunology,[3] McGill University, Montreal, Quebec, Canada H3T 1E2

Received 23 September 1999/Accepted 17 March 2000

The kissing-loop domain (KLD) encompasses a stem-loop, named kissing-loop or dimerization initiation site (DIS) hairpin (nucleotides [nt] 248 to 270 in the human immunodeficiency virus type 1 strains HIV-1_{Lai} and HIV-1_{Hxb2}), seated on top of a 12-nt stem-internal loop called stem-loop B (nt 243 to 247 and 271 to 277). Destroying stem-loop B reduced genome dimerization by ~50% and proviral DNA synthesis by ~85% and left unchanged the dissociation temperature of dimeric genomic RNA. The most affected step of reverse transcription was plus-strand DNA transfer, which was reduced by ~80%. Deleting nt 241 to 256 or 200 to 256 did not reduce genome dimerization significantly more than the destruction of stem-loop B or the DIS hairpin. We conclude that the KLD is nonmodular: mutations in stem-loop B and in the DIS hairpin have similar effects on genome dimerization, reverse transcription, and encapsidation and are also "nonadditive"; i.e., a larger deletion spanning both of these structures has the same effects on genome dimerization and encapsidation as if stem-loop B strongly impacted DIS hairpin function and vice versa. A C258G transversion in the palindrome of the kissing-loop reduced genome dimerization by ~50% and viral infectivity by ~1.4 log. Two mutations, CGCG261→UUAA261 (creating a weaker palindrome) and a Δ241–256 suppressor mutation, were each able to reduce genome dimerization but leave genome packaging unaffected.

The kissing-loop domain (KLD) encompasses a stem-loop, named kissing-loop hairpin (nucleotides [nt] 248 to 270 in human immunodeficiency virus type 1 strain HIV-1_{Lai} and HIV-1_{Hxb2} genomic RNA), seated on top of a short stem-internal loop called stem-loop B (nt 243 to 247 and 271 to 277) (18). The apical loop of the kissing-loop hairpin contains an almost invariant hexameric autocomplementary sequence (ACS) (see reference 17 and references therein), also called a palindrome. The palindrome is seen as the dimerization initiation site (DIS) of genomic RNA (13, 15, 31); thus, the kissing-loop hairpin is also called the DIS hairpin. The level of genomic RNA dimerization within isolated HIV-1 viruses is influenced by the DIS hairpin (6, 9, 17) and $p55^{Gag}$ processing (8).

In the kissing-loop model of HIV-1 genome dimerization (13, 15, 31), stem-loop B has ill-defined roles (15, 17); one might be to properly orient the DIS hairpin within the covalently linked 9,000-nt-long tangle of secondary and tertiary structure (18). Experimentally, substantial deletions within stem-loop B or the DIS hairpin have identical impacts on viral infectivity and genomic RNA encapsidation (18). This raises the possibility that the KLD might be nonmodular, i.e., a highly integrated structure whereby stem-loop B and the DIS hairpin may have similar, if not identical, physiological impacts. To establish this, it is necessary to show that stem-loop B mutations inhibit genomic RNA dimerization and proviral DNA synthesis, two processes affected by the DIS hairpin (6, 9, 17, 25).

In this paper, we identify a crucial role of stem-loop B in genome dimerization and reverse transcription and compare its physiological impact to that of the DIS hairpin. We also relate genome dimerization to viral infectivity via studying a point mutation unlikely to directly impact more than genome dimerization. The transversion C258G transforms the GCGCGC ACS into the nonpalindrome GGGCGC reduces viral infectivity by ~1.4 log [~2 logs less than larger mutations within the DIS hairpin (18)] and should not affect proviral DNA synthesis (25). Finally, we scrutinize the links between genome dimerization and genome packaging, via the study of two additional and nonoverlapping mutations. First, an ACS mutation (CGCG261→UUAA261) which preserves the palindromic nature of the ACS strongly reduces viral infectivity and in vitro dimerization of RNA transcripts, while leaving genomic RNA packaging unaffected (18). Second, a double mutation in nucleocapsid protein NCp7 and the p2 peptide partially suppresses the effects of KLD destruction, i.e., reverts genome packaging to the wild-type level and increases viral replication to a level of ~1.4 log below that of the wild-type (21, 23). We shall examine if the genomes of these two disparate and poorly infectious mutants, as well as the genome of the C258G transvertant, are poorly dimeric despite being adequately packaged.

Production of mutant viruses. COS-7 cells were transfected in parallel with equal amounts of wild-type plasmid pSVC21.BH10 and mutant plasmids such as pSVC21Δ243–247, Δ241–256, Δ200–256, LD3-MP2-MNC, GGCG, UUAA, GGCC, AGCU, Δ248–256, and Δ248–261. In pSVC21Δ243–247, CUCGG247 has been deleted; in pSVC21GGCG,

* Corresponding author. Mailing address: Lady Davis Institute for Medical Research, 3755 Cote Ste. Catherine Rd., Montreal, Quebec, Canada H3T 1E2. Phone: (514) 340-8260. Fax: (514) 340-7502. E-mail: laughrea@hotmail.com.

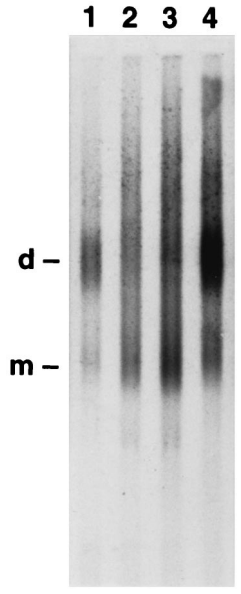

FIG. 1. Dimerization level of viral RNA isolated from BH10 (lanes 1 and 4), Δ248–256 (lane 2), and Δ243–247 (lane 3) viruses. HIV-1 genomic RNA was isolated and analyzed by nondenaturing Northern blot analysis as described previously (17). Viral RNAs were dissolved in 8 μl of buffer S (10 mM Tris [pH 7.5], 100 mM NaCl, 1 mM EDTA, 1% sodium dodecyl sulfate) and subjected to electrophoresis (70 V, 5 h 20 min, 0.7% agarose in buffer TBE_2 [Tris-borate-EDTA] at 4°C). The samples were next Northern blotted, hybridized, and autoradiographed for 8 h. d, dimer; m, monomer. Each lane represents an independent transfection and contains viral RNA isolated from 3.7 to 9 tissue culture dishes. Without a CAp24 estimate, efficiency of RNA packaging cannot be derived because of variations in virus yield from one transfection to the next. Unless otherwise indicated, the samples of Fig. 2 to 4 were processed as in Fig. 1.

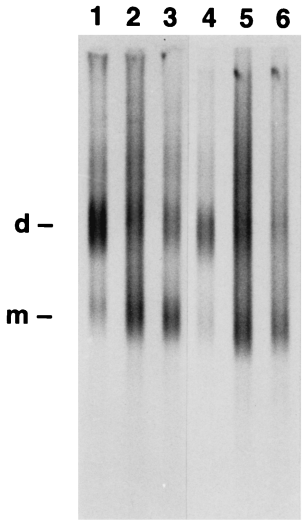

FIG. 2. Dimerization level of viral RNA isolated from BH10 (lane 1), Δ241–256 (lane 2), and LD3-MP2-MNC (lane 3) viruses, respectively, containing 8×10^{12}, 23×10^{12}, and 8×10^{12} CAp24 copies. Electrophoresis was for 5 h 15 min in 0.8% agarose. The autoradiographic exposure was for 2 h. Scanning lanes 1 to 3 and equivalent lanes from other Northern blots (not shown) indicate that Δ241–256 and LD3-MP2-MNC viruses, respectively, package genomic RNA 0.4 ± 0.08 and 0.81 ± 0.15 as well as BH10 viruses. These values are close to what was previously estimated with slot blot assays (21). Lanes 4 to 6, dimerization level of viral RNA isolated from 1.8 to 4.2 tissue culture dishes of BH10 (lane 4), Δ243–247 (lane 5), and Δ200–256 (lane 6) viruses. Electrophoresis was for 5 h 20 min in 0.7% agarose. The autoradiographic exposure was for 25 min.

CGCG261 has been replaced by GGCG—mutatis mutandis for the other plasmids. Nucleotides differing from those in HIV-1_{Lai} and HIV-1_{Mal} (subtype ADI) are underlined. The sequence of the BH10 KLD is 243CUCGGCUUGCUGAAG CGCGCACGGCAAGAGGCGAG277; nucleotides forming stem B (13) and stem C (17) (the stem of the DIS hairpin) are underlined. Comparable amounts of viruses were produced at 48 h posttransfection. To investigate the effects of the mutations on genomic RNA dimerization, genomic RNA was extracted from the isolated viruses, electrophoresed on a nondenaturating agarose gel, and detected by Northern blotting with a ^{35}S-labeled HIV-1 riboprobe (17).

Stem-loop B mutation reduces genome dimerization as much as DIS hairpin destruction. Figure 1 compares Δ243–247 genomic RNA (lane 3) to Δ248–256 (lane 2) and BH10 (lanes 1 and 4) genomic RNA. There were two similarly labeled RNA species in the Δ243–247 and Δ248–256 RNA preparations, the lower band having the same mobility as monomeric genomic RNA. Scanning lanes 1 to 4, as well as many other gel lanes from independent transfections (not shown), reveals three novel pieces of information. (i) Δ243–247 RNA was 48% ± 5% dimeric versus 85% ± 3% and 45% ± 5% dimeric for BH10 and Δ248–256 genomic RNAs. Destruction of stem-loop B had the same effect as destruction of stem C. (ii) The dimer band in the Δ243–247 and Δ248–256 samples contained 60% ± 15% more high-molecular-weight (trimer-like) complexes per unit of RNA loaded than the BH10 samples. (In BH10 RNA, the multimer shoulder amounted to 18% ± 4% of the dimer plus monomer peaks. Such shoulders are not unusual [6, 8, 9, 28].) (iii) The two mutant RNAs appeared electrophoretically diffuse as well because the trough separating the monomer and dimer peaks was not as RNA free as in the BH10 samples. To quantitate this impression, we measured, relative to the baseline of the scans, the height of the dimer peak (d), the height of the monomer peak (m), and the minimum height recorded in the trough (t). The $t/(m + d)$ ratios were, respectively, 0.3 ± 0.02 and 0.13 ± 0.03 in the mutant and BH10 samples (averaged over four to nine Northern blots). As an additional comparison, we found that genomic RNA isolated from Δ248–261 viruses (20) was 40% ± 4% dimeric and had a $t/(m + d)$ ratio of 0.25 ± 0.03 (not shown; data from five Northern blots).

Stem-loop B and stem C mutations do not have additive effects on dimerization: each is as potent as deletion of nt 200 to 256. The genomic RNA of Δ241–256 viruses was 45% ± 4% dimeric (lane 2 of Fig. 2): mutations in stem-loop B and stem C do not have additive effects on genome dimerization. Furthermore, genomic RNA from Δ200–256 viruses was 42% ± 3% dimeric (lane 6 of Fig. 2). Thus, removal of all nucleotides separating the primer binding site (PBS) (nt 182 to 199) from the ACS had no more impact than destroying stem C or stem-loop B. The Δ241–256 and Δ200–256 RNAs contained 30% ± 20% more higher-molecular-weight complexes than the BH10 samples, and their $t/(m + d)$ ratio was 0.28 ± 0.03. Hence the dimer and monomer bands were relatively diffuse.

Why does stem-loop B contribute as much to genome dimerization as the DIS hairpin, but in a nonadditive way? Stem-loop B may facilitate DIS hairpin folding (i.e., reduce the probability of alternative foldings) or orient the DIS hairpin "head" away from improper (interfering) contacts with downstream or upstream sequences, thereby increasing the probability of DIS hairpin dimerization. If genomic RNA was sufficiently shortened (sequences causing "alternative foldings" and "interfering contacts" getting deleted), the stem-loop B

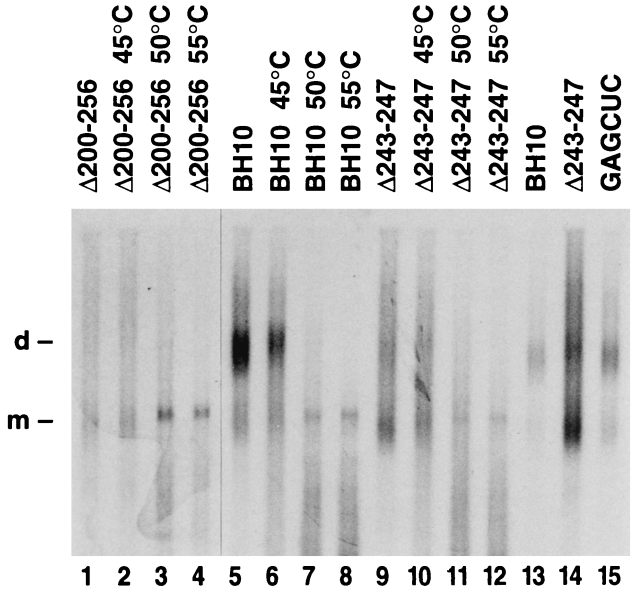

FIG. 3. Dimerization level and thermal stability of viral RNA isolated from 2.5 to 4 tissue culture dishes of the Δ200–256, BH10, and Δ243–247 viruses (lanes 1 to 12). Nonheated samples were left on ice for 10 min. The other samples were incubated in buffer S at the temperature indicated for 10 min. After incubation, all samples were loaded without delay and with the voltage on. Lanes 13 to 15 give the dimerization level of viral RNA isolated from two to eight tissue culture dishes of BH10, Δ243–247, and GAGCUC viruses (i.e., viruses whose GCGCGC262 palindrome has been replaced by GAGCUC). The autoradiographic exposures were for 6 h for lanes 1 to 4 and 3 h for lanes 5 to 15. Electrophoresis was for 4 h 30 min in 0.8% agarose.

"neck" would no longer be needed. This head-and-neck model is supported by in vitro data showing that partial HIV-1 RNA transcripts lacking nt 243 to 247 can dimerize 10 times more poorly when they end hundreds of nucleotides 3′ of the KLD than when they end <20 nt 3′ of the KLD (18). The model predicts that destruction of stem B should substantially inhibit genomic RNA dimerization, while destruction of the KLD should reduce genome dimerization no more than deletion of nt 248 to 256 or 248 to 261, which is what we found above. To reinforce this point, Fig. 3 shows that genomic RNAs from Δ200–256 (lanes 1 to 4) viruses appeared as thermostable as genomic RNA from BH10 (lanes 5 to 8) or Δ243–247 (lanes 9 to 12) viruses. BH10 RNA was monomeric at 50°C (lane 7) and 78% dimeric at 45°C (lane 6), consistent with a dissociation temperature (T_d) of ~47 to 48°C; Δ200–256 and Δ243–247 RNAs were monomeric or close to monomeric at 50°C (lanes 3 and 11) and, at 45°C, as dimeric as the unheated samples (lanes 2 and 10), consistent with a T_d of ~48 to 49°C.

C258G reduces genome dimerization as effectively as Δ200–256, without, however, generating diffuse dimer and monomer bands. We have shown that deletions of 5 to 56 nt, as long as they destroy stem-loop B or the DIS hairpin, reduce genome dimerization by half. The kissing-loop model predicts that these deletions act by obstructing ACS function. If true, transforming the ACS into a nonpalindrome via a 1-nt substitution should have a comparable impact on dimerization. Accordingly, we replaced the BH10 ACS by the GGGCGC262 nonpalindrome to generate GGCG (or C258G) viruses. Lane 2 of Fig. 4 shows that genomic RNA from C258G viruses was 50% dimeric. Scanning this and several other C258G gel lanes (not shown) revealed that the mutant genomic RNA was 48% ± 4% dimeric, versus 44% dimeric for the average deletion mutant, and 42% dimeric for Δ200–256 RNA (see above; e.g., compare lane 2 of Fig. 4 to lane 6 of Fig. 2). The $t/(m + d)$ ratio (0.16 ± 0.02) and the multimer content (17% ± 3%) of C258G RNA were as low as those in BH10 RNA. C258G represents the smallest molecular change ever shown to affect HIV genomic RNA dimerization.

As a control, we engineered a C258G suppressor mutation, i.e., replaced the BH10 ACS by GGGCCC262, a theoretically valid palindrome nevertheless absent from all sequenced HIVs and simian immunodeficiency viruses (SIVs) (12, 18). The genome of the double transvertant viruses was 83% ± 3% dimeric (i.e., wild-type like [data not shown]). The infectivity of the double transvertant was not significantly impaired (18), supporting the idea that wild-type infectivity requires wild-type levels of genome dimerization.

Good packaging stoichiometry but poor dimerization: three examples. Replacing the BH10 ACS by GUUAAC leaves genomic RNA packaging unaffected (18). Lane 3 of Fig. 4 shows that genomic RNA from UUAA viruses was half-dimeric and appeared as well-resolved dimer and monomer bands. Scans of this and other UUAA lanes (not shown) revealed that UUAA RNAs were 55% ± 4% dimeric and had a $t/(m + d)$ ratio of 0.15 ± 0.02 and a multimer content of 21% ± 2% (i.e., were electrophoretically indistinguishable from C258G RNAs). Northern blot analyses (intensity of the monomer and dimer bands per unit of CAp24 loaded) confirmed that UUAA viruses packaged genomic RNA as well as BH10 (Fig. 4). UUAA genomic RNA was much less dimeric than genomic RNA from AGCU viruses (lane 15 of Fig. 3). AGCU is absent from the palindromes of all HIVs and SIVs so far sequenced (12, 16), while UUAA is found in the putative DIS hairpin of SIV_{mnd} (18).

Point mutations T24I in NCp7 and T12I in the p2 peptide suppress the deletion of nt 241 to 256 in three ways. (i) Genome packaging is boosted from ~30% to ≥80% of the wild-type level (21 [see below]). (ii) Viral replication is boosted by at least 2 logs (21 [see below]). (iii) The maturation kinetics of the CAp24-p2 protein into CAp24 and p2 seems to be ≥70% restored (22). (The name of the Δ241–256 suppressor is LD3-

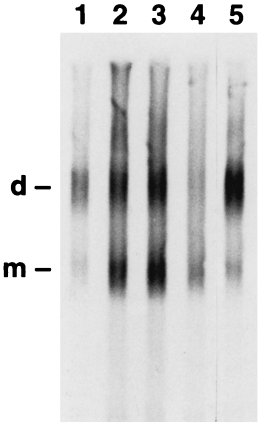

FIG. 4. Dimerization level of viral RNA isolated from BH10 (lane 1), GGCG (lane 2), UUAA (lane 3), and Δ248–256 (lane 4) viruses containing 1.3×10^{12}, 5×10^{12}, 5×10^{12}, and 4×10^{12} CAp24 copies. GGCG viruses have a C258G transversion. UUAA viruses have CGCG261 replaced by UUAA. Lane 5, dimerization level of viral RNA isolated from BH10 viruses containing 4×10^{12} CAp24 copies. Electrophoresis was for 4 h 35 min in 1% agarose. The autoradiographic exposure was for 1 h. Scanning of lanes 1 to 3 and equivalent lanes from other Northern blots indicates that GGCG, UUAA, and Δ248–256 viruses, respectively, package genomic RNA 0.78 ± 0.12, 1.1 ± 0.11, and 0.4 ± 0.06 as well as BH10 viruses. These numbers are consistent with previous estimates using dot blot assays (18).

MP2-MNC, with LD3 being a designation for Δ241–256.) However, lane 3 of Fig. 2 shows that genomic RNA from LD3-MP2-MNC viruses was 42% dimeric. The average over several Northern blots was 43% ± 6%, undistinguishable from the 45% ± 4% obtained with Δ241–256 viruses. The NCp7 and p2 suppressor mutations failed to suppress the Δ241–256 defect in genome dimerization. On the other hand, the ratio $t/(m + d)$ and the multimer content of LD3-MP2-MNC RNA were wild-type like (lane 3 of Fig. 2 [not shown]). Northern blot analyses confirm that LD3-MP2-MNC viruses packaged genomic RNA almost as well as BH10 viruses (Fig. 2).

Finally, Northern blot analyses suggest that C258G viruses packaged genomic RNA 78% ± 12% as well as BH10 viruses (Fig. 4). This is consistent with a previous report showing that two palindrome point mutations (G261U and GCGCGC 262→GGGGGG262) did not grossly reduce genomic RNA packaging in virions (6).

These three convergent observations do not necessarily mean that genome packaging has in all respects been dissociated from genome dimerization: a KLD-independent signal might exist which stimulates cytoplasmic formation of dimers prone to dissociate during genomic RNA extraction or electrophoresis. Conversely, the C258G, UUAA, and LD3-MP2-MNC RNAs packaged in the mutant viruses may have been monomeric prior to protease-directed maturation of $p55^{Gag}$ (8). In addition, we cannot strictly exclude the idea that the majority (~60 to 65%) of the three mutant viruses contained one genomic RNA per 50% smaller protein shell: the diameter, surface (CAp24 content), and packaging efficiency (number of genomic RNAs per unit of CAp24) of these small viruses would, respectively, be ~79, ~63, and ~79% of those of BH10. However HIV-1 viruses severely deficient in packaging do not appear significantly smaller than the wild type (1, 5). Finally, even if the mutant viruses could consistently package two genomic RNAs per protein shell, assembling a protein shell around two monomeric genomic RNAs (or a dimer lacking a functional KLD) might be kinetically slower than assembling it around one fully dimeric BH10 genome.

If losing KLD-directed genome dimerization does not inhibit packaging, why were Δ241–256 viruses encapsidation defective? Δ241–256 viruses may have lost two independent signals: a dimerization signal and a separate packaging signal. We imagine that the T24I mutation in the NCp7 of LD3-MP2-MNC viruses compensates for the latter loss by enhancing some form of genomic RNA binding beyond the capacity of BH10 NCp7 (described below).

Heterogenous migration of genomic RNAs from packaging-defective viruses: do they form complexes with subgenomic RNA? Δ243–247, Δ241–256, Δ248–256, and Δ248–261 viruses were packaging defective (Fig. 2 and 4) (17, 18), and their RNA bands were diffuse (above). In contrast, C258G, UUAA, and LD3-MP2-MNC viruses packaged genomic RNA ~90% as well as BH10 on average (Fig. 2 and 4) and presented sharp RNA bands. Since the amount of spliced viral RNA inside viruses mutated in the KLD is the same as that in wild-type viruses (6), if not larger (24), KLD mutants encapsidating half as well as BH10 should contain, per genomic RNA, two to four times more spliced viral RNA than BH10 viruses or KLD mutants encapsidating as well as BH10. If a large proportion of the RNAs moving as a shoulder behind the dimer band, and halfway between dimers and monomers, were dimers and monomers hybridized to subgenomic RNA(s), then a doubling or tripling of spliced viral RNAs per genomic RNA in Δ243–247, Δ241–256, Δ248–256, and Δ248–261 viruses might significantly increase the proportion of genomic RNAs moving as a shoulder behind the dimer band and halfway between dimers and monomers. This could explain why in Northern blots from these viruses, the relative height of the multimer shoulder was increased by ~45% and the relative RNA content in the trough separating the monomer and the dimer band was increased ~2.2-fold.

Partial reduction in genome dimerization may cause a 25-fold reduction in viral infectivity. Using the 50% tissue culture infective dose method (17), we performed infectivity tests on, respectively, two and three independent preparations of LD3-MP2-MNC and Δ241–256 viruses: the logs of BH10 titer/mutant titer were, respectively, 1.35 ± 0.3 and 4.2 ± 0.5 (not shown) versus 1.45 ± 0.25 and 1.35 ± 0.25 for the C258G and UUAA viruses (18). The Δ241–256 and LD3-MP2-MNC titers confirm and extend similar titers independently obtained by Liang et al. (23). LD3-MP2-MNC viruses are thus 11- to 50-fold less infectious than the wild type (20- to 25-fold on average), and they have a phenotype apparently indistinguishable from that of C258G and UUAA viruses, despite the nonoverlapping nature of the mutations: identical low infectivity, identically deficient genome dimerization, and little or no impact on genome packaging and other functions. It is tempting to suggest that the poor genome dimerization displayed by the C258G, UUAA, and LD3-MP2-MNC strains causes their poor infectivity. If true, reducing genomic RNA dimerization by 50% would reduce viral infectivity ~25-fold and at most 50-fold.

Stem-loop B mutation reduces proviral DNA production as much as DIS hairpin destruction. In the hope of discovering why destruction of stem-loop B inhibits dimerization no more than the C258G transversion, but reduces viral infectivity by ~3.4 logs (18), we analyzed viral DNA present inside 2.5×10^6 MT-2 cells infected with equal amounts of DNase I-treated BH10 and mutant viruses, each containing 25 ng of CAp24 (17). Intracellular DNA harvested 10 h after infection (10, 11, 29, 38) was subjected to 25 cycles of PCR (7) with primer pairs designed to amplify β-globin DNA (27) and different regions of proviral DNA (20). Serial dilutions of pSVC21.BH10 linearized with Spe1 served to quantitate intracellular proviral DNA and acted as a control for PCR linearity. The β-globin gene acted as an internal control. The Δ248–256 and Δ248–261 data were pooled together as representing, for comparative purposes, DIS hairpin destruction (Table 1). We used primers pR and pU5′ (Table 1) to quantitate DNA containing the RU5 sequence (i.e., minus-strand strong-stop DNA plus subsequent DNAs), primers pPBS and pMA′ (Table 1 caption) to quantitate DNA containing the PBS-to-MA (matrix) DNA sequence (9.1-kb minus-strand DNA [Table 1] plus subsequent DNAs), and primers pR and pMA′ to quantitate nearly complete proviral DNA.

The intracellular quantity of nearly complete proviral DNA was decreased ~15-fold when BH10 viruses were replaced by viruses mutated in stem-loop B or the DIS hairpin (pR-pMA′ column of Table 1). After correction for poor genome packaging, the mutant reverse transcriptional machinery appeared approximately eightfold less productive than BH10, as if the stem-loop B and DIS hairpin poles of the KLD interfered strongly and equally with production of nearly complete proviral DNA. Is this inhibition due to decreased DNA synthesis or increased degradation? Assuming increased degradation leads to a difficulty. At 10 h postinfection, the RU5 and PBS-MA DNA would be minimally degraded (Table 1), while the more freshly synthesized R-MA DNA (merely RU5 and PBS-MA DNA linked via a 14-nt linker) would be extensively degraded prior to PCR: one would have to suppose that the 14-nt linker is about 50 times more labile, per nucleotide res-

TABLE 1. Mutant proviral DNA present in infected MT2 cells as a percentage of wild-type proviral DNA, 10 h after infection,[a] and specific impact of stem-loop B and DIS hairpin destruction on early, intermediate, and late events of reverse transcription

Mutant	% of wild-type DNA with primer pairs:				
	pR-pMA′	pPBS-pMA′	pR-pU5′ (~early events[b])	pPBS-pMA′/pR-pU5′ (~intermediate events[c])	pR-pMA′/pPBS-pMA′ (~late events[d])
Δ243–247	12 ± 4 (7 ± 2)	65 ± 30 (40 ± 20)	80 ± 20 (45 ± 12)	80 ± 45	18 ± 11
Δ248–256 and Δ248–261[e]	13 ± 6 (8 ± 4)	60 ± 15 (36 ± 10)	75 ± 25 (45 ± 15)	80 ± 35	22 ± 11
Control (BH10)	100[f] (100)	100[g] (100)	100[h] (100)	100	100

[a] PCR was performed as described in the text. Primers pR (5′ AGA CCA GAT CTG AGC CTG GGA G35) and pMA′ (CT GAC GCT CTC GCA CCC [the antisense of nt 338 to 354]), respectively, hybridize to the minus strand of R DNA and to the plus strand of matrix DNA. Primers pPBS and pU5′ (5′ CCA CAC TGA CTA AAA GGG TC [the antisense of nt 148 to 167]), respectively, hybridize to the minus strand of the PBS and to the plus strand of U5 DNA. For pR-pMA′, pPBS-MA′, and pR-pU5′, the amount of mutant proviral DNA per unit of β-globin DNA was divided by the amount of wild-type proviral DNA per unit of β-globin DNA, multiplied by 100, and corrected for deficient genomic RNA packaging in the mutant viruses (18). Values in parentheses are the numbers obtained before correction for deficient genomic RNA packaging. No correction was made for the presumed two- to fourfold-higher proportion of subgenomic RNA present in the mutant viruses (6, 24). This correction would have been negligible with primer pairs pR-pMA′ and pPBS-pMA′ (PCR signal lost by hypothetical transfer of minus-strand strong-stop DNA from the genomic to subgenomic strand would have been almost completely regained by transfer of minus-strand strong-stop DNA from the subgenomic to genomic strand) and small with the primer pair pR-pU5′ (see footnote *b*).

[b] This reflects or exaggerates the specific effect of the mutations on minus-strand strong-stop DNA production (maximum extension of minus-strand DNA prior to minus-strand transfer). Why "exaggerates"? A worst-case scenario follows. Assume that all wild-type proviral DNA synthesis was completed at 10 h (doubtful), while mutant proviral DNA synthesis was unaffected at the level of minus-strand strong-stop DNA synthesis, but 100% blocked at the level of minus-strand transfer (clearly not the case). A mutant PCR yield of 25% of the wild-type level would be reported, because each mutant proviral DNA would have been single stranded (with one pR/pU5′ binding site), while wild-type proviral DNA would have contained two LTRs (and thus would have had four pR/pU5′ binding sites). If wild-type proviral DNA synthesis was completed at 10 h while mutant proviral DNA synthesis was 100% blocked at the level of plus-strand transfer (not quite the case), a mutant PCR yield of 50% of the wild-type level would be reported (because of one LTR per mutant DNA versus two in the wild type). On the other hand, the higher relative proportion of subgenomic RNAs expected in Δ243–247, Δ248–256, and Δ248–261 viruses will increase this 50% yield to 55 to 59% (assuming 0.2 to 0.3 subgenomic RNAs per genomic RNA in mutant viruses versus 0.1 in wild-type viruses). Let's now describe a reasonable scenario: if BH10 proviral DNA synthesis was 90% completed at 10 h while mutant proviral DNA synthesis was 80% blocked at the level of plus-strand transfer (last column) and mutant viruses contained 0.3 subgenomic RNA per genomic RNA versus 0.1 in wild-type viruses (see references 6 and 24 and the text), a mutant PCR yield of 76% of BH10 proviral DNA synthesis would obtain (64% in the absence of correction for differential packaging of spliced viral RNAs). Interestingly, this matches the percentage reported in the column. This modeling and the attending uncertainties should not distract from the main experimental result: stem-loop B and DIS hairpin mutations have indistinguishable effects on reverse transcription. Also, the fact that the pR-pU5′ column yields averages above 50% suggests that production of plus-strand strong-stop DNA is not affected in the mutant viruses.

[c] This division reflects or possibly underestimates by a factor of ~2 the aggregate effect of the mutations on minus-strand transfer plus formation of 9.1-kb minus-strand DNA (maximum extension of minus-strand DNA produced prior to plus-strand transfer). Indeed, since the percentage expressed in the pR-pU5′ column may reflect more than the effect of mutations on minus-strand strong-stop cDNA synthesis (see above), it follows that dividing the pPBS-pMA′ column by the pR-pU5′ column may underestimate the effect of the mutations on minus-strand transfer plus formation of 9.1-kb minus-strand DNA.

[d] This division reflects the aggregate effect of the mutations on a mixture of late events, including initiation of plus-strand DNA synthesis, plus-strand transfer, and displacement of the minus strand of the 5′ LTR by the nascent extension of 9.1-kb minus-strand DNA.

[e] The effects of deleting nt 248 to 261 or 248 to 256 were insignificantly different. With each set of primers, Δ248–256 viruses were actually on average slightly less productive than Δ248–261 viruses, consistent with the idea that the ACS does not influence proviral DNA synthesis (25).

[f] On average, there were ~2,000 apparent DNA copies per 10^5 cells. At 2 h postinfection, there were <50 apparent DNA copies per 10^5 cells. One apparent DNA copy is the amount of proviral DNA giving the same PCR signal as one linearized SVC21.BH10 plasmid. The actual number depends on the number of PCR primer binding sites in the nascent proviral DNA relative to the number of PCR primer binding sites in linearized SVC21.BH10.

[g] On average, there were ~2,000 apparent DNA copies per 10^5 cells. At 2 h posttransfection, there were ~400 apparent DNA copies per 10^5 cells.

[h] On average, there were ~4,000 apparent DNA copies per 10^5 cells. At 2 h posttransfection, there were ~2,000 apparent DNA copies per 10^5 cells.

idue, than flanking sequences. We conclude that our mutations are more likely to affect DNA synthesis than DNA degradation.

A late step of reverse transcription is preferentially inhibited. After correction for lower encapsidation, it was not clear that RU5 DNA production was decreased (pR-pU5′ column of Table 1), and PBS-MA DNA production was not dramatically reduced (pPBS-pMA′ column of Table 1), indicating that the destruction of stem-loop B preferentially impaired a step located between production of 9.1-kb minus-strand DNA and nearly complete proviral DNA (Table 1). Specifically, the steps leading from 9.1-kb minus-strand DNA to nearly complete proviral DNA were inhibited 70 to 90% (last column of Table 1), whereas all previous steps were inhibited less, if at all (pPBS-pMA′ column of Table 1). Total cellular DNA harvested at 2 h postinfection gave PCR results consistent with the 10-h data. PCR at 10 and 2 h postinfection measures intraviral plus intracellular proviral DNA production (2, 26, 35, 39–41). Subtraction of the 2-h data from the 10-h data yields intracellular DNA production during the 8-h interval: we found that the ratios of mutant to BH10 production, after correction for RNA packaging, were very close to those reported in Table 1, namely ~0.6 with primer pairs pR-pU5′ and pPBS-pMA′ and ~0.15 with primer pair pR-pMA′ (not shown).

Choking between synthesis of 9.1-kb minus-strand DNA and nearly complete proviral DNA could have three causes (34): (i) step A, poor formation of plus-strand strong-stop DNA (maximum extension of plus-strand DNA produced before plus-strand transfer). (This could be due to excessive degradation of the polypurine track, deficient initiation of plus-strand DNA synthesis, deficient DNA-directed elongation, poor displacement of the PBS RNA strand still hybridized to $tRNA_3^{Lys}$ [3], or premature degradation of $tRNA_3^{Lys}$.); (ii) step B, poor plus-strand transfer per se, i.e., poor annealing between plus-strand PBS DNA and minus-strand PBS DNA (This could be due to step Bi, poor accessibility of plus-strand PBS DNA because of slow degradation of $tRNA_3^{Lys}$ (32), or step Bii, poor accessibility of minus-strand PBS DNA.); (iii) step C, poor displacement of the minus strand of the 5′ long terminal repeat (LTR) (4).

Working hypothesis: KLD mutations result in a minus-strand PBS DNA folding which hinders annealing with plus-strand PBS DNA. KLD RNA cannot directly influence steps B and C, because it should by then be degraded. Even though plus-strand strong-stop DNA is probably made sometime before 9.1-kb minus-strand DNA (34, 36), a direct effect of KLD RNA on a step A seems unlikely; in addition, the relatively abundant accumulation of plus-strand strong-stop DNA in the cytoplasm of infected cells (34) suggests that formation of plus-strand strong-stop DNA is not rate limiting in plus-strand

transfer. Minus-strand KLD DNA cannot influence steps A and Bi, because they are expected to precede its appearance (34). An effect solely on step C is ruled out, because blocking it would inhibit R-MA DNA production (relative to PBS-MA DNA production) by only 50% (because plus-strand DNA elongation would remain unhindered) versus the ~80% reported in Table 1; in addition, we can't easily conceptualize how minus-strand KLD DNA could affect 5′ LTR strand displacement. An effect on step Bii is easier to imagine: mutant minus-strand KLD DNA, located only 43 nt upstream of minus-strand PBS DNA, might stimulate an aberrant minus-strand PBS DNA folding that hinders annealing with plus-strand PBS DNA. This model can be tested with a reconstituted reverse transcription system (38).

Nonobvious factors influencing late steps of reverse transcription. Vif protein (30, 37), NCp7, and the KLD are three nonobvious factors which can affect reverse transcription steps posterior to minus-strand strong-stop DNA production. NCp7 from HIV-1_{MN} stimulates annealing between plus-strand PBS DNA and minus-strand PBS DNA, at least in the context of proviral DNAs truncated before KLD DNA (38), and NCp7 from HIV-1_{NL43} may stimulate strand displacement posterior to plus-strand transfer (33). These NCp7 proteins, like those from LD3-MP2-MNC virus, have an Ile24 in their N-terminal zinc finger; only HIV-1_{Hxb2}, the source of BH10 viruses, and two subtype D viruses have a Thr24 in their NCp7 (12). Thus, NCp7 from LD3-MP2-MNC viruses is in this regard more conformist than wild-type NCp7 from BH10 and Δ241–256 viruses. Perhaps HIV-1_{Hxb2} is slightly underendowed in strand annealing and genomic RNA packaging: this underendowment may become rate limiting in the context of a Δ241–256 deletion presumed to inhibit packaging in a dimerization-independent manner and to hinder annealing of plus-strand PBS DNA to minus-strand PBS DNA.

This work was supported by grant MT-12312 from the Medical Research Council of Canada to M. Laughrea.

REFERENCES

1. **Aldovini, A., and R. A. Young.** 1990. Mutations of RNA and protein sequences involved in human immunodeficiency virus type 1 packaging result in production of noninfectious virus. J. Virol. **64:**1920–1926.
2. **Arts, E. J., J. Mak, L. Kleiman, and M. A. Wainberg.** 1994. DNA found in human immunodeficiency virus type 1 may not be required for infectivity. J. Gen. Virol. **75:**1605–1613.
3. **Ben-Artzi, H., J. Shemesh, E. Zeelon, B. Amit, L. Kleiman, M. Gorecki, and A. Panet.** 1996. Molecular analysis of the second template switch during reverse transcription of the HIV RNA template. Biochemistry **35:**10549–10557.
4. **Boone, L. R., and A. M. Skalka.** 1993. Strand displacement synthesis by reverse transcriptase, p. 119–133. *In* A. M. Skalka and S. P. Goff (ed.), Cold Spring Harbor Laboratory Press, Cold Spring Harbor, N.Y.
5. **Clavel, F., and J. M. Orenstein.** 1990. A mutant of human immunodeficiency virus with reduced RNA packaging and abnormal particle morphology. J. Virol. **64:**5230–5234.
6. **Clever, J. L., and T. G. Parslow.** 1997. Mutant human immunodeficiency virus type 1 genomes with defects in RNA dimerization or encapsidation. J. Virol. **71:**3407–3414.
7. **Dieffenbach, C. W., and G. S. Dveksler (ed.).** 1995. PCR primer, a laboratory manual. Cold Spring Harbor Laboratory Press, Cold Spring Harbor, N.Y.
8. **Fu, W., R. J. Gorelick, and A. Rein.** 1994. Characterization of human immunodeficiency virus type 1 dimeric RNA from wild-type and protease-defective virions. J. Virol. **68:**5013–5018.
9. **Haddrick, M., A. L. Lear, A. J. Cann, and S. Heaphy.** 1996. Evidence that a kissing loop structure facilitates genomic RNA dimerization in HIV-1. J. Mol. Biol. **259:**58–68.
10. **Hahn, B. H., G. M. Shaw, S. K. Arya, M. Popovic, R. C. Gallo, and F. Wong-Staal.** 1984. Molecular cloning and characterization of the HTLV-III virus associated with AIDS. Nature **312:**166–169.
11. **Kim, S., R. Byrn, J. Groopman, and D. Baltimore.** 1989. Temporal aspects of DNA and RNA synthesis during human immunodeficiency virus infection: evidence for differential gene expression. J. Virol. **63:**3708–3713.
12. **Korber, B., C. Kuiken, B. Foley, B. Hahn, F. McCutchan, J. W. Mellors, and J. Sodroski (ed.).** 1998. Human retroviruses and AIDS. Los Alamos National Laboratory, Los Alamos, N.Mex.
13. **Laughrea, M., and L. Jetté.** 1994. A nineteen nucleotide sequence upstream of the 5′ major splice donor is part of the dimerization domain of the HIV-1 genome. Biochemistry **33:**13464–13475.
14. **Laughrea, M., and L. Jetté.** 1996. Kissing-loop model of HIV-1 genome dimerization: HIV-1 RNAs can assume alternative dimeric forms and all sequences upstream or downstream of hairpin 248-271 are dispensable for dimer formation. Biochemistry **35:**1589–1598.
15. **Laughrea, M., and L. Jetté.** 1996b. HIV-1 genome dimerization: formation kinetics and thermal stability of dimeric HIV-1*Lai* RNAs are not improved by the 1-232 and 296-790 regions flanking the kissing-loop domain. Biochemistry **35:**9366–9374.
16. **Laughrea, M., and L. Jetté.** 1997. HIV-1 genome dimerization: kissing-loop hairpin dictates whether nucleotides downstream of the 5′ splice junction contribute to loose and tight dimerization of human immunodeficiency virus RNA. Biochemistry **36:**9501–9508.
17. **Laughrea, M., L. Jetté, J. Mak, L. Kleiman, C. Liang, and M. A. Wainberg.** 1997. Mutations in the kissing-loop hairpin of human immunodeficiency virus type 1 reduce viral infectivity as well as genomic RNA packaging and dimerization. J. Virol. **71:**3397–3406.
18. **Laughrea, M., N. Shen, L. Jetté, and M. A. Wainberg.** 1999. Variant effects of non-native kissing-loop hairpin palindromes on HIV replication and HIV RNA dimerization: role of stem-loop B in HIV replication and HIV RNA dimerization. Biochemistry **38:**226–234.
19. **Li, X., J. Mak, E. J. Arts, Z. Gu, L. Kleiman, M. A. Wainberg, and M. A. Parniak.** 1994. Effects of alterations of primer-binding site sequences on human immunodeficiency virus type 1 replication. J. Virol. **68:**6198–6206.
20. **Liang, C., X. Li, L. Rong, P. Inouye, Y. Quan, L. Kleiman, and M. A. Wainberg.** 1997. The importance of the A-rich loop in human immunodeficiency virus type 1 reverse transcription and infectivity. J. Virol. **71:**5750–5757.
21. **Liang, C., L. Rong, M. Laughrea, L. Kleiman, and M. A. Wainberg.** 1998. Compensatory point mutations in the human immunodeficiency virus type 1 Gag region that are distal from deletion mutations in the dimerization initiation site can restore viral replication. J. Virol. **72:**6629–6636.
22. **Liang, C., L. Rong, E. Cherry, L. Kleiman, M. Laughrea, and M. A. Wainberg.** 1999. Deletion mutagenesis within the dimerization initiation site of human immunodeficiency virus type 1 results in delayed processing of the p2 peptide from precursor proteins. J. Virol. **73:**6147–6151.
23. **Liang, C., L. Rong, Y. Quan, M. Laughrea, L. Kleiman, and M. A. Wainberg.** 1999. Mutations within four distinct Gag proteins are required to restore replication of human immunodeficiency virus type 1 after deletion mutagenesis within the dimerization initiation site. J. Virol. **73:**7014–7020.
24. **McBride, M. S., and A. T. Panganiban.** 1997. Position dependence of functional hairpins important for human immunodeficiency virus type 1 RNA encapsidation in vivo. J. Virol. **71:**2050–2058.
25. **Paillart, J.-C., L. Berthoux, M. Ottmann, J.-L. Darlix, R. Marquet, B. Ehresmann, and C. Ehresmann.** 1996. Dual role of the putative RNA dimerization initiation site of human immunodeficiency virus type 1 in genomic RNA packaging and proviral DNA synthesis. J. Virol. **70:**8348–8354.
26. **Quan, Y., L. Rong, C. Liang, and M. A. Wainberg.** 1999. Reverse transcriptase inhibitors can selectively block the synthesis of differently sized viral DNA transcripts in cells acutely infected with human immunodeficiency virus type 1. J. Virol. **73:**6700–6707.
27. **Saiki, R. K., S. Scharf, F. Faloona, K. B. Mullis, G. T. Horn, H. A. Erlich, and N. Arnheim.** 1985. Enzymatic amplification of beta-globin genomic sequences and restriction site analysis for diagnosis of sickle cell anemia. Science **230:**1350–1354.
28. **Sakuragi, J.-I., and A. T. Panganiban.** 1997. Human immunodeficiency virus type 1 RNA outside the primary encapsidation and dimer linkage region affects RNA dimer stability in vivo. J. Virol. **71:**3250–3254.
29. **Sambrook, J., E. F. Fritsch, and T. Maniatis.** 1989. Molecular cloning: a laboratory manual, 2nd ed. Cold Spring Harbor Laboratory Press, Cold Spring Harbor, N.Y.
30. **Simon, J. H., and M. H. Malim.** 1996. The human immunodeficiency virus type 1 Vif protein modulates the postpenetration stability of viral nucleoprotein complexes. J. Virol. **70:**5297–5305.
31. **Skripkin, E., J.-C. Paillart, R. Marquet, B. Ehresmann, and C. Ehresmann.** 1994. Identification of the primary site of the human immunodeficiency virus type 1 RNA dimerization in vitro. Proc. Natl. Acad. Sci. USA **91:**4945–4949.
32. **Smith, C. M., J. S. Smith, and M. J. Roth.** 1999. RNase H requirements for the second strand transfer reaction of human immunodeficiency virus type 1 reverse transcription. J. Virol. **73:**6573–6581.
33. **Tanchou, V., D. Decimo, C. Péchoux, D. Lener, V. Rogemond, L. Berthoux, M. Ottmann, and J.-L. Darlix.** 1998. Role of the N-terminal zinc finger of human immunodeficiency virus type 1 nucleocapsid protein in virus structure and replication. J. Virol. **72:**4442–4447.
34. **Telesnitsky, A., and S. P. Goff.** 1993. Strong-stop strand transfer during reverse transcription, p. 49–84. *In* A. M. Skalka and S. P. Goff (ed.), Cold

Spring Harbor Laboratory Press, Cold Spring Harbor, N.Y.
35. **Trono, D.** 1992. Partial reverse transcripts in virions from human immunodeficiency and murine leukemia viruses. J. Virol. **66:**4893–4900.
36. **Varmus, H. E., S. Heasley, H.-J. Kung, H. Opperman, V. C. Smith, J. M. Bishop, and P. R. Shank.** 1978. Kinetics of synthesis, structure and purification of avian sarcoma virus-specific DNA made in the cytoplasm of acutely infected cells. J. Mol. Biol. **120:**55–82.
37. **von Schwedler, U., J. Song, C. Aiken, and D. Trono.** 1993. *vif* is crucial for human immunodeficiency virus type 1 proviral DNA synthesis in infected cells. J. Virol. **67:**4945–4955.
38. **Wu, T., J. Guo, J. Bess, L. E. Henderson, and J. G. Levin.** 1999. Molecular requirements for human immunodeficiency virus type 1 plus-strand transfer: analysis in reconstituted and endogenous reverse transcription systems. J. Virol. **73:**4794–4805.
39. **Zhang, H., Y. Zhang, T. P. Spicer, L. Z. Abbott, M. Abbott, and B. J. Poiesz.** 1993. Reverse transcription takes place within extracellular HIV-1 virions: potential biological significance. AIDS Res. Hum. Retrovir. **9:**1287–1296.
40. **Zhang, H., O. Bagasra, M. Niikura, B. J. Poiesz, and R. J. Pomerantz.** 1994. Intravirion reverse transcripts in the peripheral blood plasma of human immunodeficiency virus type 1-infected individuals. J. Virol. **68:**7591–7597.
41. **Zhang, H., G. Dornadula, and R. J. Pomerantz.** 1996. Endogenous reverse transcription of human immunodeficiency virus type 1 in physiological microenvironments: an important stage for viral infection of nondividing cells. J. Virol. **70:**2809–2824.